

Propagation of polarised light in bent hi-bi spun fibres

Ya.V. Przhiyalkovsky, S.K. Morshnev, N.I. Starostin, V.P. Gubin

Abstract. The evolution of polarisation states (PS's) of broadband light propagating through a bent optical fibre with a helical structure of its refractive index anisotropy (hi-bi spun fibre) has been studied theoretically and experimentally. It has been shown that there exists a coordinate system of PS's in which the differential Jones matrix can be replaced by a diagonal matrix, which allows the polarisation parameters of the output broadband light to be readily calculated with sufficient accuracy. We have derived a formula for evaluating the magneto-optical sensitivity of a bent spun fibre. An approach has been proposed for restoring the degree of polarisation of light in a bent hi-bi spun fibre and, as a consequence, the visibility (contrast) of the interferometer in a current sensor with a sensing element based on the fibre under consideration.

Keywords: bent hi-bi spun fibre, polarisation, current sensor.

1. Introduction

Electric current measurements by an optical method using magnetic field-sensitive optical fibres with a helical structure of their refractive index anisotropy (hi-bi spun fibres) are of interest for electric power generation and electrometallurgy. The key component of the sensing element (SE) in Faraday effect fibre-optic current sensors (FOCS's) [1] is a loop consisting of one or a few turns of hi-bi spun fibre, and a wire carrying an electric current to be measured passes through the plane of the loop. Hi-bi spun fibres are produced by drawing a preform with a built-in linear birefringence (BR), which is rapidly spun during the drawing process. The performance of SEs depends on the parameters of the spun fibre: the beat length of the built-in linear BR of the fibre (L_b) and the spin pitch of its helical structure (L_{tw}). To improve the resistance of sensing elements to mechanical deformation, it is reasonable to use fibre with high BR (small beat length L_b). The performance of sensing elements depends, in particular, on the bend radius of the fibre when it is wound: with decreasing R , the magneto-optical sensitivity S of the spun fibre decreases and, no less importantly, the visibility of the interference pattern of the current sensor drops considerably, which limits the dynamic range of electric current measurements from below.

The properties of bent spun fibre have been the subject of several studies [1–3]. Laming and Payne [1] were the first to propose using hi-bi spun fibre in sensing elements of Faraday effect current sensors and present a phenomenological formula for sensitivity S as a function of R , which was verified experimentally within a 2% change in sensitivity.

Gubin et al. [2] and Polynkin and Blake [3] reported the first theoretical studies of the effect of fibre bending on the parameters of the sensing element of FOCS's. Gubin et al. [2] proposed a physical model for bent spun fibre and, using numerical integration of a differential Jones matrix, assessed the magneto-optical sensitivity of the fibre. They obtained an analytical expression for the Faraday phase shift between two light waves in a straight spun fibre segment. As shown in Refs [2, 3], under excitation with circularly polarised light the Faraday phase shift accumulation (i.e. magneto-optical sensitivity) has an oscillating nature along the length of the fibre, with a large and a small spatial period, and the oscillation amplitude increases with decreasing bend radius. According to Polynkin and Blake [3], for a certain input polarisation state (PS), dependent on the parameters and bend radius of the fibre, the large-period oscillations disappear.

Note that the above-mentioned studies analysed monochromatic light. In real FOCS's, however, use is made of broadband light. In analysis of light propagation in spun fibre, the bandwidth of the light has so far been taken into account only for a straight fibre segment [4, 5]. This circumstance indicates that the properties of bent spun fibre have not yet been studied in sufficient detail. Also, there are no analytical formulas applicable in a wide range of SE diameters.

In this paper, we present an analytical approach to describing the PS of both monochromatic and broadband light propagating through bent spun fibre. The approach allows one to calculate wavelength-averaged parameters of the PS and the magneto-optical sensitivity of the fibre. The limitations we place on the parameters of the spun fibre and the winding radius are beyond the ranges of these parameters in real FOCS's. The approach is a development of theory considered previously [4] for a straight spun fibre segment and involves a search for such a coordinate system for representing the PS of light in which the differential Jones matrix of bent spun fibre can to some approximation be replaced by a diagonal matrix at each point of the fibre. This means that, in the case of bent spun fibre, one can also calculate parameters of the wavelength-averaged PS of the output light and magneto-optical sensitivity, similarly to what was reported previously [4]. The theory developed by us has made it possible to propose a method for restoring the contrast of the interference pattern in the interferometer of FOCS's.

Ya.V. Przhiyalkovsky, S.K. Morshnev, N.I. Starostin, V.P. Gubin
V.A. Kotelnikov Institute of Radio Engineering and Electronics
(Fryazino Branch), Russian Academy of Sciences, pl. Vvedenskogo 1,
141190 Fryazino, Moscow region, Russia; Profotech CJSC,
Vereiskaya ul. 17, 121357 Moscow, Russia;
e-mail: yankus.p@gmail.com, nis229@ire216.msk.su

Received 24 March 2015

Kvantovaya Elektronika 45 (11) 1075–1082 (2015)

Translated by O.M. Tsarev

2. Principles of theoretical analysis of spun fibres

To describe the PS of a light wave propagating in optical fibres, use is often made of the differential Jones matrix formalism. The evolution of the Jones vector representing the PS of light can be described by the differential equation

$$\frac{d\mathbf{E}}{dz} = N\mathbf{E}, \quad (1)$$

where \mathbf{E} is the Jones vector formed by the complex amplitudes of the electric field components of the wave and N is the differential Jones matrix of the optical fibre.

In a circular polarisation basis, the differential Jones matrix of a uniformly bent spun fibre segment has the form [2]

$$N_c(z) = \begin{pmatrix} i\frac{\gamma}{2} & i\frac{\beta}{2}e^{-i2\xi z} + i\frac{\delta}{2}e^{-i2\nu} \\ i\frac{\beta}{2}e^{i2\xi z} + i\frac{\delta}{2}e^{i2\nu} & -i\frac{\gamma}{2} \end{pmatrix}, \quad (2)$$

where γ is the rate of the increase in the Faraday effect-induced phase difference between waves with orthogonal circular polarisations; $\beta = k_y - k_x = 2\pi/L_b$ is the rate of the increase in the phase difference between waves with orthogonal linear polarisations due to built-in linear BR with a beat length L_b ; $\xi = 2\pi/L_{tw}$ is the spatial rotation frequency of the axes of built-in linear BR with a spin pitch L_{tw} ; $\delta = 2\pi/L_{ind}$ is the rate of the increase in the phase difference between waves with orthogonal linear polarisations due to bend-induced BR with a beat length L_{ind} [2]; ν is the azimuth of the bend-induced BR axes at the input fibre end relative to the built-in BR axes; and z is a coordinate along the fibre axis.

To describe the PS of light, it is convenient to utilise its representation on the Poincare sphere [6]. In a circular polarisation basis, the poles of the Poincare sphere represent circular PS's, and the points on its equator represent linear PS's with various azimuths. The constant-latitude circles, parallel to the equator, represent the set of PS's of constant ellipticity, and the constant-longitude arcs represent PS's of constant azimuth.

In what follows, we use the auxiliary matrices

$$T_1 = \begin{pmatrix} e^{i\alpha/2} & 0 \\ 0 & e^{-i\alpha/2} \end{pmatrix}, \quad T_2 = \begin{pmatrix} \cos(\varphi/2) & \sin(\varphi/2) \\ -\sin(\varphi/2) & \cos(\varphi/2) \end{pmatrix}. \quad (3)$$

These matrices will be considered as transformation matrices of the coordinate system of PS's, namely, as rotation matrices of the Poincare sphere. The T_1 matrix represents a rotation of the sphere through an angle α about the Z axis of three-dimensional space containing the sphere, and the T_2 matrix represents a rotation of the sphere through an angle φ about the Y axis (Fig. 1). The inverse matrices of T_i ($i = 1, 2$) are then equivalent to rotations through negative angles: $T_i^{-1}(\alpha) = T_i(-\alpha)$.

3. Substantiation of the choice of the coordinate system for analysing the PS of bent fibre

In examining the evolution of the PS of light in a straight spun fibre, it is often convenient to use a so-called rotating coordinate system of PS's (which rotates as the z coordinate increases along the fibre), or a helical coordinate system of space. In

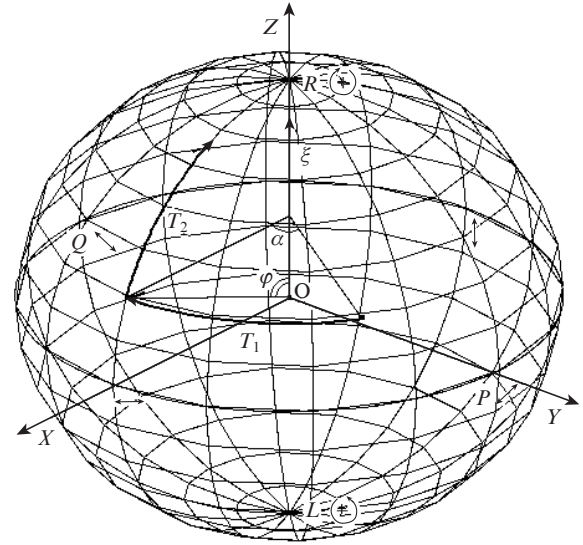


Figure 1. Rotations of the T_1 and T_2 matrices of the Poincare sphere.

this coordinate system, basis PS's are orthogonal PS's whose ellipticity (equal to the eigenellipticity [4]) is determined by the parameters of the fibre and whose azimuths are identical to the azimuths of the vectors of the BR axes at a given point, i.e. vary linearly with increasing distance along the fibre.

This coordinate system of PS's is convenient in that the differential matrix of a straight spun fibre in this system has a diagonal form at each of its points, so the equations of evolution can readily be integrated. This means that the evolution of the PS of an excitation light wave is represented on the Poincare sphere particularly simply: with increasing distance from the input fibre end, the representative point of the PS uniformly moves on the sphere along a trajectory whose points are equidistant from the basis PS's, i.e. along a circumference. At the same time, in the case of broadband light the spatial velocity of motion along such a circumference is wavelength-dependent, so some distance from the input fibre end the points representing the PS's of all the spectral components of the input light fill an entire circumference. Owing to this simple geometric distribution of the points representing PS's, one can readily obtain the average parameters of the light at the fibre output: from the fact that the PS's of the spectral components of light are equidistant from the points representing the basis PS's, it follows that the average ellipticity is equal to the ellipticity of the basis PS's and that the average azimuth is equal to the azimuth of one of the basis PS's, depending on the PS of the input light. This can be used to calculate the magneto-optical sensitivity (determined by the average ellipticity) of the spun fibre under consideration, which is used in SEs of current sensors [4]. It is also easy to calculate the degree of light polarisation, which determines the interferometer contrast, depends on parameters of the PS of the input light and can be found as the distance from the centre of the sphere to the plane containing the circumference with the points representing the PS when the radius of the sphere is unity.

In the case of a bent spun fibre, the differential equations of the evolution of the PS are equivalent to a Riccati equation [2], which generally cannot be integrated. This means that, generally speaking, there is no such coordinate system of PS's in which the differential Jones matrix has a diagonal form at

each point of the fibre. It can be shown however that there is a coordinate system of PS's in which, to some approximation, the same situation occurs as in examining a straight spun fibre in a rotating coordinate system: the point representing the PS of a light wave moves along a trajectory which is nearly equidistant from the points representing the basis PS's. This means that, in the case of a bent spun fibre, one can also calculate, to the approximation in question, the parameters of the wavelength-averaged PS of the output light and the magneto-optical sensitivity of the fibre. The coordinate system in question is represented by the following transformation matrix:

$$E_c = T(z)E_c = T_2(\varphi_2)T_1(\alpha_2)T_2(\varphi_1)T_1(\alpha_1)E_c. \quad (4)$$

The former pair of rotations in (4) (the same as in the case of a straight spun fibre) comprises sequential rotations through an angle α_1 about the Z axis and through an angle φ_1 about the Y axis of space containing the Poincare sphere (Fig. 1):

$$\alpha_1(z) = 2\xi z, \quad \tan \varphi_1 = \frac{\beta}{2\xi} = \frac{L_{tw}}{2L_b}. \quad (5)$$

The latter pair comprises the same sequence of rotations, but through the following angles:

$$\alpha_2(z) = -2(\xi z - v), \quad \varphi_2 = \varphi_2(z), \quad (6)$$

where $\varphi_2(z)$ generally depends on the z coordinate.

Differentiating (4) and using (1) we obtain an equation for the evolution of the PS in the new coordinate system:

$$\frac{dE_c}{dz} = N_c(z)E_c. \quad (7)$$

Here the differential Jones matrix is expressed through the corresponding matrix in the laboratory coordinate system of PS's as follows:

$$N_c(z) = \frac{dT}{dz}T^{-1} + TN_cT^{-1}. \quad (8)$$

Making algebraic calculations, we can obtain an expression for the differential Jones matrix in the new coordinate system:

$$N_c(z) = \frac{i}{2} \times \begin{pmatrix} Y \cos(\mu - \varphi_2) & Y \sin(\mu - \varphi_2) - i(\varphi_2' + Q) \\ Y \sin(\mu - \varphi_2) + i(\varphi_2' + Q) & -Y \cos(\mu - \varphi_2) \end{pmatrix}, \quad (9)$$

where

$$\begin{aligned} Y &= \sqrt{W^2 + P^2}; \quad \tan \mu = P/W; \\ P &= \delta \{ \cos \varphi_1 \cos^2 [2(\xi z - v)] + \sin^2 [2(\xi z - v)] \}; \\ Q &= -\delta \frac{1 - \cos \varphi_1}{2} \sin [4(\xi z - v)]; \\ W &= \Omega - 2\xi + \delta \sin \varphi_1 \cos [2(\xi z - v)]; \end{aligned} \quad (10)$$

$$\Omega = \sqrt{(2\xi + \gamma)^2 + \beta^2};$$

and φ_2' is the derivative of the function $\varphi_2(z)$ with respect to the z coordinate.

The angle φ_2 has not yet been determined. To understand how to determine φ_2 , consider the behaviour of the function μ . It is seen from (10) that μ is expressed through periodic functions, so it is also periodic. An idea of how to determine φ_2 is seen from the form of matrix (9): this angle can be determined as the period-averaged μ (with a slight displacement due to oscillations in the amplitude of Y). The $\cos(\mu - \varphi_2)$ in the diagonal matrix elements will then oscillate around unity, and the off-diagonal elements will oscillate around zero, because $\sin(\mu - \varphi_2)$ and Q oscillate around zero and, as shown below, φ_2' is either zero or negligible in the context of the problem under consideration.

Consider now the function $Y \sin(\mu - \varphi_2)$ in greater detail. To simplify the formulas below, we use the following designations:

$$\tilde{\sigma} = \frac{\delta}{\Omega - 2\xi} \frac{1 + \cos \varphi_1}{2}, \quad (11a)$$

$$\tilde{Q} = \sqrt{(\Omega - 2\xi)^2 + \delta \left(\frac{1 + \cos \varphi_1}{2} \right)^2} = (\Omega - 2\xi) \sqrt{1 + \tilde{\sigma}^2}. \quad (11b)$$

Substituting (10) into $Y \sin(\mu - \varphi_2)$, we obtain

$$\begin{aligned} Y \sin(\mu - \varphi_2) &= \delta \cos \varphi_2 \frac{1 + \cos \varphi_1}{2} - (\Omega - 2\xi) \sin \varphi_2 \\ &- \delta \sin \varphi_1 \sin \varphi_2 \cos [2(\xi z - v)] - \delta \frac{1 - \cos \varphi_1}{2} \\ &\times \cos \varphi_2 \cos [4(\xi z - v)]. \end{aligned} \quad (12)$$

It is seen that the difference between the first two terms in Eqn (12), which is independent of z , is zero if the angle φ_2 is determined as follows:

$$\tan \varphi_2 = \tilde{\sigma}. \quad (13)$$

Similarly, taking into account (13) we obtain for the function $Y \cos(\mu - \varphi_2)$

$$\begin{aligned} Y \cos(\mu - \varphi_2) &= \tilde{Q} + \delta \sin \varphi_1 \cos \varphi_2 \cos [2(\xi z - v)] \\ &- \delta \frac{1 - \cos \varphi_1}{2} \sin \varphi_2 \cos [4(\xi z - v)]. \end{aligned} \quad (14)$$

Finally, the differential matrix can be represented as a sum:

$$N_c = N_c^0 + V_1 + V_2 + V_Q = N_c^0 + V, \quad (15)$$

where

$$\begin{aligned} N_c^0 &= \frac{i}{2} \tilde{Q} \begin{pmatrix} 1 & 0 \\ 0 & -1 \end{pmatrix}; \\ V_1 &= \frac{i}{2} \delta \sin \varphi_1 \begin{pmatrix} \cos \varphi_2 & \sin \varphi_2 \\ \sin \varphi_2 & -\cos \varphi_2 \end{pmatrix} \cos [2(\xi z - v)]; \\ V_2 &= \frac{i}{2} \delta \frac{1 - \cos \varphi_1}{2} \begin{pmatrix} -\sin \varphi_2 & -\cos \varphi_2 \\ -\cos \varphi_2 & \sin \varphi_2 \end{pmatrix} \cos [4(\xi z - v)]; \end{aligned} \quad (16)$$

$$V_Q = \frac{i}{2} \varphi' \begin{pmatrix} 0 & -i \\ i & 0 \end{pmatrix} - \frac{i}{2} \delta \frac{1 - \cos \varphi_1}{2} \begin{pmatrix} 0 & -i \\ i & 0 \end{pmatrix} \sin[4(\xi z - v)].$$

All the above transformations were rigorous. As pointed out above, the starting equations generally have no analytical solution, so a number of assumptions will be made in what follows. We seek an approximate solution to the basic equation (7), using time-dependent perturbation theory and treating N_e^0 as a matrix describing the unperturbed system and V_1 , V_2 and V_Q as a perturbation. We then have an analogy with a classic problem for a two-level system with an interlevel transition frequency $\tilde{\Omega}$ (in our case, the levels are the propagation constants of waves with basis PS's, and frequencies are spatial). It is seen from matrices (16) that the spatial frequencies of perturbations are 2ξ and 4ξ . Therefore, if the spatial frequency $\tilde{\Omega}$ differs strongly from these frequencies (as shown below, this is so for the parameters of fibre and bend radii used in practice), perturbations have no significant effect and can be neglected in the approximation in question.

Consider now two types of fibre bends: a constant-radius bend and a bend with a gradually varying radius. Analysis of a constant-radius bend is of great importance for understanding the evolution of the PS of light waves in a bent fibre, but in practice the bend radius is difficult to maintain constant throughout a fibre, including its ends. Moreover, it is important to take into account the azimuthal orientations of the input light, fibre axes and winding plane. The latter case (a bend with a gradually varying radius) is simpler in terms of experimental verification and practical application.

4. Spun fibre with a constant bend radius

In the case of a constant bend radius, $\delta = \text{const}$ and hence $\varphi_2' = 0$. The starting equation of evolution in an elliptic coordinate system of PS's has the form

$$\frac{d\mathbf{E}}{dz} = (N_e^0 + V)\mathbf{E}. \quad (17)$$

(here and in what follows, the subscript e at the Jones vector is omitted to simplify the notation).

We seek an approximate solution using time-dependent perturbation theory and treating V_1 , V_2 and V_Q as perturbations in a problem represented by the N_e^0 matrix:

$$\frac{d\mathbf{E}^0}{dz} = N_e^0 \mathbf{E}^0. \quad (18)$$

Equation (18) can readily be integrated and the general solution has the form of a linear combination of independent solutions:

$$\mathbf{E}^0 = C_1 \mathbf{E}_u^0 + C_2 \mathbf{E}_v^0, \quad (19)$$

where

$$\mathbf{E}_u^0 = \exp\left(i \frac{\tilde{\Omega} z}{2}\right) \begin{pmatrix} 1 \\ 0 \end{pmatrix}; \quad \mathbf{E}_v^0 = \exp\left(-i \frac{\tilde{\Omega} z}{2}\right) \begin{pmatrix} 0 \\ 1 \end{pmatrix}. \quad (20)$$

The general solution to the starting equation (17) can be represented as solution (19) with the coefficients C_1 and C_2 dependent on the z coordinate:

$$\mathbf{E} = C_1(z) \mathbf{E}_u^0 + C_2(z) \mathbf{E}_v^0. \quad (21)$$

We seek C_i ($i = 1, 2$) in the form of the expansion $C_i = C_i^0 + C_i^1$, where C_i^0 is the zero-order term, which is independent of perturbation, and the coefficient C_i^1 is a linear function of the perturbation. Let only the E_u component of light be excited at the input fibre end. Then, we have

$$C_1(z) = 1 + C_1^1(z), \quad C_2(z) = C_2^1(z). \quad (22)$$

Performing algebraic calculations by a standard procedure of perturbation theory, we can obtain an approximate solution to the starting equation:

$$E_u \approx \exp\left(i \frac{\tilde{\Omega} z}{2}\right) \left\{ 1 + \frac{i}{2} \int_0^z \left[\delta \sin \varphi_1 \cos \varphi_2 \cos[2(\xi z - v)] + \delta \frac{1 - \cos \varphi_1}{2} \sin \varphi_2 \cos[4(\xi z - v)] \right] dz \right\}. \quad (23)$$

After integration, the terms on the right-hand side of (23) will be proportional to $\delta/(2\xi) = L_{\text{tw}}/(2L_{\text{ind}})$. In practice, this ratio is very small because L_{tw} is typically 3–5 mm, which is far less than L_{ind} (for example, at a fibre diameter of 125 μm and winding radius of 4 mm we have $L_{\text{ind}} \sim 50$ mm). Integrating (23) and taking into account that, since the integrals are small, the term in curly brackets in (23) can be thought of as an expansion of an exponential function, we obtain after integration

$$E_u \approx \exp\left[i \frac{(\tilde{\Omega} + \Delta\tilde{\Omega})z}{2}\right], \quad (24)$$

where

$$\Delta\tilde{\Omega} = \frac{1}{z} \frac{\delta}{2\xi} \left\{ \sin \varphi_1 \cos \varphi_2 \{ \sin[2(\xi z - v)] + \sin(2v) \} + \frac{1 - \cos \varphi_1}{2} \sin \varphi_2 \{ \sin[4(\xi z - v)] + \sin(4v) \} \right\}. \quad (25)$$

Similarly, the E_v component of the solution can be represented as follows:

$$E_v = \exp\left(-i \frac{\tilde{\Omega} z}{2}\right) \frac{i}{2} \int_0^z \left\{ \delta \sin \varphi_1 \sin \varphi_2 e^{i\tilde{\Omega} z} \cos[2(\xi z - v)] - \delta \frac{1 - \cos \varphi_1}{2} \cos \varphi_2 e^{i\tilde{\Omega} z} \cos[4(\xi z - v)] - i\delta \frac{1 - \cos \varphi_1}{2} e^{i\tilde{\Omega} z} \sin[4(\xi z - v)] \right\} dz. \quad (26)$$

Integrating (26), we obtain summands divided by the sums and differences of the frequencies $\tilde{\Omega}$ and 2ξ or 4ξ , because these integrals are bounded Fourier transforms of the corresponding functions at frequency $\tilde{\Omega}$. Consider how these frequencies are related to each other. To this end, we examine the relation

$$\frac{\tilde{\Omega}}{2\xi} = (\sqrt{\sigma^2 + 1} - 1)\sqrt{\sigma^2 + 1} = \sqrt{\left(\frac{\delta}{2\xi}\right)^2 + (\sqrt{\sigma^2 + 1} - 1)^2}. \quad (27)$$

The ratio is determined by the latter term, because the former is small. It is seen that, for $\sigma < 1.5$ (which is fulfilled in most

practical cases: e.g., at $L_{tw} = 3$ mm, we have $L_b > 1$ mm), the inequality $\tilde{\Omega} < 2\xi < 4\xi$ is satisfied. Therefore, after integration of (26) the largest term will be that proportional to the coefficient $\delta/(2\xi - \tilde{\Omega})$, whose magnitude (at $\sigma = 1.5$) is

$$\delta/(2\xi - \tilde{\Omega}) \approx 5\delta/(2\xi) \ll 1. \tag{28}$$

Thus, we are led to conclude that, for $L_{tw}/(2L_{ind}) \ll 1$ and $\sigma = L_{tw}/(2L_b) < 1.5$, the perturbation in Eqn (17) has no significant effect, so solution (20) to the unperturbed problem (18) can be used in the initial problem with good accuracy.

The fact that, in this approximation, the differential matrix can be thought of as having a diagonal form [N_e^0 in (16)] allows us to draw important conclusions as to the evolution of the PS. In such a coordinate system, the PS of a light wave moves along a circumference equidistant from the basis PS's on the Poincare sphere. In the case of broadband light, some distance from the input fibre end (coherence length) the points representing the PS's of light waves throughout the spectrum of the input light begin to fill an entire circumference, so the degree of light polarisation as a function of parameters of the input PS can be found as the distance from the centre of the Poincare sphere to the plane containing the circumference with the PS's of the waves [4]. The wavelength-averaged ellipticity is then equal to the ellipticity of the basis PS's and the average azimuth is equal to the azimuth of one of the basis PS's. It is therefore important to know the evolution of the basis PS's of the elliptic coordinate system, whose motion can be represented in the laboratory coordinate system of circular PS's from Eq. (4), by substituting, e.g., vector u of the polarisation mode

$$E_{cu}(z) = T_1(-\alpha_1) T_2(-\varphi_1) T_1(-\alpha_2) T_2(-\varphi_2) \begin{pmatrix} 1 \\ 0 \end{pmatrix} \tag{29}$$

into this equation.

It is seen from (29) and (3) that the Jones vector is periodic, so the motion trajectory is a closed curve. If there is no bend, the trajectory has the form of a constant-latitude circumference (Fig. 2a) corresponding to an eigenellipticity with a linearly increasing azimuth [4]. With increasing δ (decreasing bend radius), the trajectory tilts towards the bend BR vector and the shape of the curve begins to distort and differ from a circumference (Fig. 2b). The ellipticity begins to oscillate at a frequency 2ξ , the ellipticity averaged over the period $L_{tw}/2$ drops, and the azimuth increases with increasing z , also with some oscillations. After a certain value of δ is reached, the trajectory of the evolution of the basis PS on the Poincare sphere passes through a circular PS. The ellipticity then con-

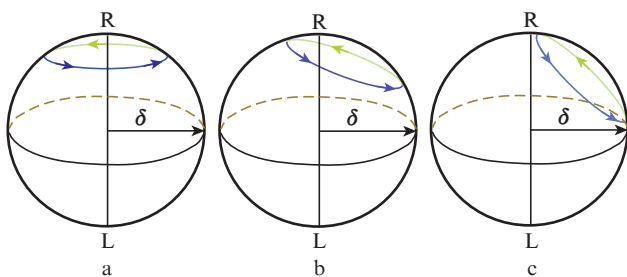


Figure 2. Trajectories of the evolution of a basis PS of an elliptic coordinate system at different bend radii.

tinues to oscillate with a larger amplitude around a lower period-averaged value, and the azimuth stops infinitely increasing and begins to oscillate around an average value equal to the azimuth of the bend BR vector (Fig. 2c). Thus, the ellipticity averaged over the oscillation period $L_{tw}/2$ decreases with decreasing fibre winding radius.

Differential magneto-optical sensitivity is defined as the increase in the phase difference between u and v polarisation modes when the coefficient γ changes by $d\gamma$ over a fibre section of length dz :

$$S = \frac{d^2}{d\gamma dz} (\tilde{\Omega}z + \Delta\tilde{\Omega}) = S_{av} + \frac{d^2}{d\gamma dz} \Delta\tilde{\Omega}. \tag{30}$$

The latter term in (30) represents oscillations around zero. Since the phase difference between the u and v polarisation modes is obtained by integration over all dz segments, this term does not contribute to the final phase difference, so the integrated sensitivity is only determined by S_{av} . Differentiating (11b), we obtain

$$S_{av} = \frac{d\tilde{\Omega}}{d\gamma} = S_e S_b, \tag{31}$$

where

$$S_e = \frac{1}{\sqrt{\sigma^2 + 1}}; \tag{32a}$$

$$S_b = \frac{1}{\sqrt{\delta^2 + 1}}. \tag{32b}$$

Thus, the magneto-optical sensitivity of fibre comprises two factors, one of which is determined by the eigenellipticity of the fibre and is equal to the sensitivity of a straight spun fibre [4] and the other is determined by the bend.

Note that the integrated sensitivity of a current sensor with a spun fibre-based SE depends not only on its intrinsic magneto-optical sensitivity but also on the number of fibre turns wound around a current-carrying conductor and the Verdet constant of the fibre material. Note that, with decreasing winding radius, S decreases, whereas the number of turns around a current-carrying conductor at a fixed spun-fibre length increases. Figure 3 presents a calculated final dependence of the sensitivity of a current sensor on the winding

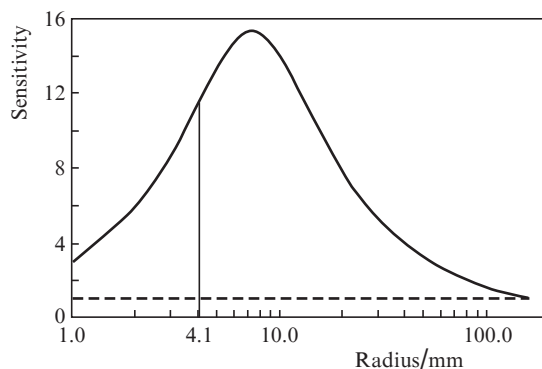


Figure 3. Calculated integrated sensitivity as a function of bend radius (solid line) for a 1-m-long spun-fibre segment; $L_{tw} = 3$ mm, $L_b = 11$ mm. The dashed line shows the sensitivity for one turn with $R = 159$ mm.

radius. It is seen that, down to minimum radii, the increase in sensitivity due to the increase in the number of turns upon a decrease in winding radius surpasses the drop in magneto-optical sensitivity, which justifies the use of SEs at a small spun-fibre winding radius [e.g. at $R = 4.1$ mm, sensitivity is 11.5 times that for one turn with $R = 1/(2\pi)$ m ≈ 159 mm].

5. Spun fibre with a varying bend radius

It can be shown that, if the bend radius varies smoothly enough, the polarisation evolution at each point of the fibre is, to some accuracy, the same as in the case of a constant winding radius corresponding to R at a given point.

Let the winding radius and, hence, the coefficient δ be functions of fibre length: $\delta = \delta(z)$. An additional perturbation then emerges, which is determined by the derivative φ'_2 [see (16)]:

$$\varphi'_2 = \frac{\delta'}{\delta} \frac{\sin(2\varphi_2)}{2}. \quad (33)$$

It should be taken into account that, in this case, δ in expressions (23) and (26) for components of a wave cannot be pulled out of the integral sign and that the term $i\varphi'_2 e^{i\Omega z}$ appears under the integral sign in the expression for E_v in (26). As above, E_u is represented by (24), where

$$\Delta\tilde{\Omega} = \frac{1}{z} \int_0^z \left[\delta \sin\varphi_1 \cos\varphi_2 \cos[2(\xi z - \nu)] + \delta \frac{1 - \cos\varphi_1}{2} \sin\varphi_2 \cos[4(\xi z - \nu)] \right] dz, \quad (34)$$

and the expression for E_v comprises bounded Fourier transforms of the corresponding functions at the frequency $\tilde{\Omega}$. Therefore, for this component to be small the length scale of variations in δ should far exceed the period $2\pi/\tilde{\Omega}$. The polarisation component E_u will then not convert into the orthogonal one.

When a bent fibre is used in practice as a sensing element of a current sensor, the u and v polarisation modes should be working light waves of the interferometer in order to maintain a high degree of polarisation and, hence, the contrast of the entire interferometer. To produce these modes and ensure reflection from a mirror into the orthogonal mode, appropriate phase plates should be placed at the input and output fibre ends in the same way as in the case of straight fibre described previously [5]. At the same time, in the case of bent fibre the polarisation parameters of input light also depend on the radius and orientation of the winding plane, which should be taken into account for reflection of light from the mirror at the output fibre end. This adds complexity to the fabrication of the input and output phase plates and is extremely inconvenient in practice.

For this reason, in the case of practical application of a sensitive loop with a small spun-fibre winding radius in a current sensor, it is more convenient to use such a loop configuration in which the radius at the loop input gradually decreases from a large one, at which the effect of fibre bend can be neglected, to the desired one, whereas the radius at the loop output varies in the opposite way. The input and output phase plates will then be identical to those in the case of a straight spun fibre [5].

Note that if L_b is several times greater than L_{tw} , the input phase plate approaches a $\lambda/4$ plate, and the output plate has a negligible effect on the PS (see [5]), it is permissible to use a conventional SE configuration with a $\lambda/4$ phase plate at its input and a mirror at its output.

6. Interferometer contrast and magneto-optical sensitivity measurements

The conclusion that the degree of polarisation remains unchanged in the case of gradual fibre bending was verified as follows: A sensing element with different fibre winding configurations was connected to a FOCS [2], and the interference pattern contrast was measured, first at $R = 100$ mm and then with the entire spun fibre wound onto a small-radius silica tube (Fig. 4a). Next, about 2 m of the fibre was wound off at both ends and coiled in the form of a spiral next to the fibre wound onto the tube (Fig. 4b).

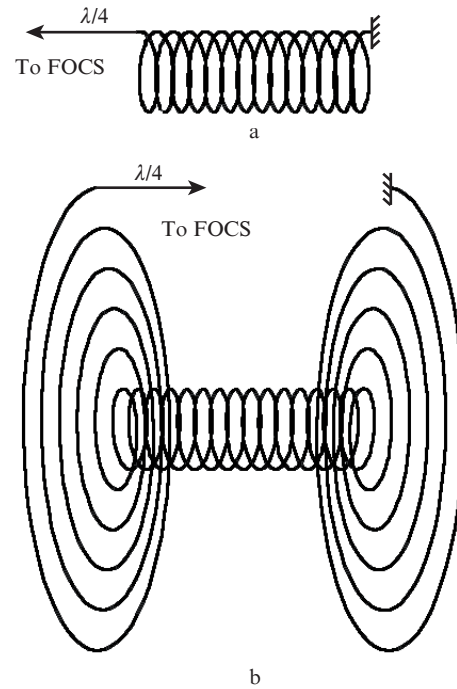


Figure 4. Schematics of the sensing element of a current sensor: (a) traditional, (b) with a gradual decrease in winding radius at the input fibre end and a gradual increase at the output end.

In our experiments, we used three 125- μ m-diameter hi-bi spun fibre samples: with an elliptical stress cladding and initial parameters $L_b = 21 \pm 1$ mm and $L_{tw} = 3.0 \pm 0.5$ mm (spun-1); with an elliptical core, $L_b = 11 \pm 1$ mm and $L_{tw} = 3.0 \pm 0.5$ mm (spun-2); and bow-tie fibre with $L_b = 10.8 \pm 0.5$ mm and $L_{tw} = 4.8 \pm 0.5$ mm (spun-3). The measurement results are presented in Figs 5a, 5c and 5e. The experiments confirmed that, in the proposed scheme, high contrast was maintained at small loop winding radii.

To assess magneto-optical sensitivity [see formulas (31), (32a) and (32b)], a predetermined reference current was measured using a FOCS [2] and an SE based on the fibre under investigation. First, we used an SE with a large (200 mm) spun fibre winding diameter, at which the effect of

bending on its sensitivity was negligible. Next, the fibre was wound as shown in Fig. 4b. Spiral winding allowed us to compare measurements at similar contrast values and ruled out any effect of contrast on measurement results. The relative sensitivity due to the bend was calculated as the ratio of the measured currents normalised to one turn in the configurations schematised in Figs 4a and 4b [the coefficient representing eigenellipticity in (32a) is then cancelled out]. The measurement results for spun-1, spun-2 and spun-3 are presented in Figs 5b, 5d and 5f. The slight discrepancy between the experimental data and calculated curve for the spun-1 sample in Fig. 5b can be accounted for by difficulties in the experiments with this sample, because it exhibited

high sensitivity to external mechanical influences due to its low built-in BR.

7. Conclusions

The evolution of polarisation states of light has been examined theoretically for light propagation through a hi-bi spun fibre coiled along a circumference of arbitrary radius and placed in a magnetic field. Using the differential Jones matrix formalism, an approximate solution to the equation of PS evolution has been obtained analytically for fibre parameters and bend radii typically used in practice. It has been shown

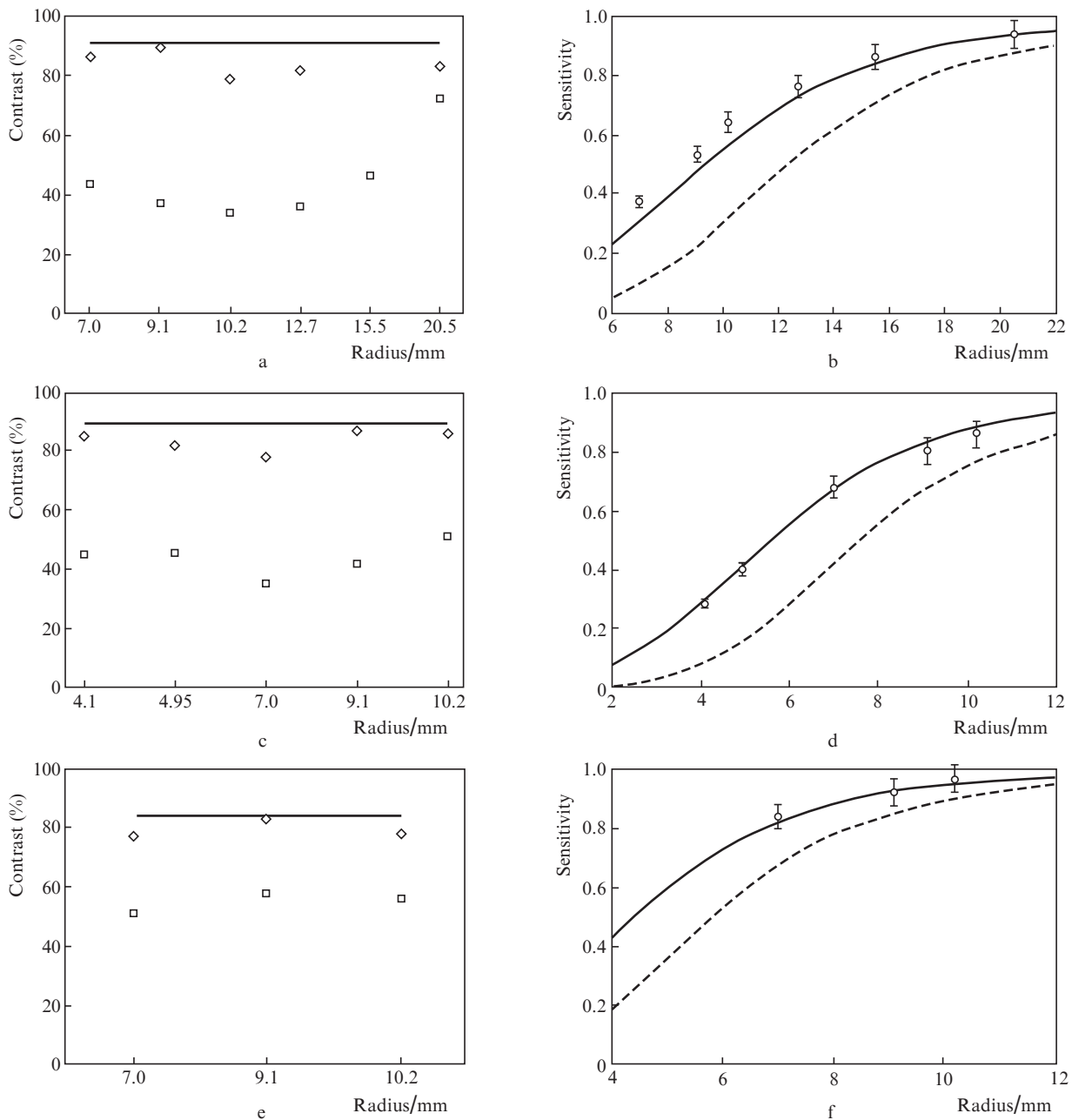


Figure 5. Interferometer contrast as a function of fibre bend radius for the (a) spun-1, (c) spun-2 and (e) spun-3 fibres (squares: constant-radius fibre winding; diamonds: fibre winding with two spiral sections; straight line: straight spun fibre) and sensitivity as a function of fibre winding radius [circles: measurement results; solid line: theoretical curve obtained using formula (32b) and the following parameters: (b) $L_b = 20$ mm, $L_{tw} = 3.5$ mm; (d) $L_b = 11$ mm, $L_{tw} = 3$ mm; (f) $L_b = 11$ mm, $L_{tw} = 4.8$ mm; (spun-3); dashed lines: calculation [1] for the same parameters].

that there exists a coordinate system of PS's in which, to some approximation, a situation holds analogous to that for a straight spun fibre in a local (rotating) coordinate system in which the differential Jones matrix has a diagonal form and equations can be solved exactly. In the coordinate system in question, the differential Jones matrix of a bent spun fibre can be represented as the sum of a diagonal matrix and perturbation matrices, which allows one to find an approximate solution to such a system using time-dependent perturbation theory. We have determined fibre parameters and bend radii at which spatial perturbation frequencies and the frequency of transitions between basis PS's differ strongly (this is the case for fibre and bend parameters typically used in practice), which allows perturbations to be neglected. Therefore, in the case of a bent spun fibre, one can also analytically calculate, to the indicated approximation, polarisation parameters (ellipticity, azimuth, and degree of polarisation) of the wavelength-averaged PS of the output light and the magneto-optical sensitivity of the fibre. We have considered a gradual variation in bend radius when the degree of polarisation of light remains unchanged.

The proposed theory has been used to derive a formula for evaluating the magneto-optical sensitivity of a bent spun fibre. An approach has been proposed for restoring the degree of polarisation of light in a bent spun fibre and, as a consequence, the interference pattern contrast in a Faraday effect current sensor. The approach relies on the fact that, if the spun fibre bend radius varies smoothly enough, the associated perturbations do not create conditions for light depolarisation in the fibre. The proposed configuration of the sensing element of a current sensor includes fibre sections (spirals) with a varying winding radius at its input and output. Theoretical conclusions have been confirmed experimentally. We have demonstrated visibility improvement from 40% to 90% at minimum winding radii in the range 4.1–20.5 mm.

References

1. Laming R.I., Payne D.N. *J. Lightwave Technol.*, **7**, 2084 (1989).
2. Gubin V.P., Isaev V.A., Morshnev S.K., et al. *Kvantovaya Elektron.*, **36** (3), 287 (2006) [*Quantum Electron.*, **36** (3), 287 (2006)].
3. Polynkin P., Blake J. *J. Lightwave Technol.*, **23**, 3815 (2005).
4. Przhiyalkovsky Ya.V., Morshnev S.K., Starostin N.I., Gubin V.P. *Kvantovaya Elektron.*, **43** (2), 167 (2013) [*Quantum Electron.*, **43** (2), 167 (2013)].
5. Przhiyalkovsky Ya.V., Morshnev S.K., Starostin N.I., Gubin V.P. *Kvantovaya Elektron.*, **44** (10), 957 (2014) [*Quantum Electron.*, **44** (10), 957 (2014)].
6. Azzam R.M.A., Bashara N.M. *Ellipsometry and Polarised Light* (Amsterdam–New York–Oxford: North-Holland Publ. Comp., 1977).